Journal of
Materials Chemistry B

Accepted Manuscript

This is an *Accepted Manuscript*, which has been through the RSC Publishing peer review process and has been accepted for publication.

Accepted Manuscripts are published online shortly after acceptance, which is prior to technical editing, formatting and proof reading. This free service from RSC Publishing allows authors to make their results available to the community, in citable form, before publication of the edited article. This *Accepted Manuscript* will be replaced by the edited and formatted *Advance Article* as soon as this is available.

To cite this manuscript please use its permanent Digital Object Identifier (DOI®), which is identical for all formats of publication.

More information about *Accepted Manuscripts* can be found in the **Information for Authors**.

Please note that technical editing may introduce minor changes to the text and/or graphics contained in the manuscript submitted by the author(s) which may alter content, and that the standard **Terms & Conditions** and the **ethical guidelines** that apply to the journal are still applicable. In no event shall the RSC be held responsible for any errors or omissions in these *Accepted Manuscript* manuscripts or any consequences arising from the use of any information contained in them.

Cite this: DOI: 10.1039/c0xx00000x

www.rsc.org/xxxxxx

ARTICLE TYPE

Chemically tunable cationic polymer-bonded magnetic nanoparticles for gene magnetofection

Makoto Takafuji,[a,b] Kumiko Kitaura,[a] Takuro Nishiyama,[a] Srinath Govindarajan,[c] Vijaya Gopal,[c] Takashi Imamura,[a,d] and Hirotaka Ihara[a,b*]

Received (in XXX, XXX) Xth XXXXXXXXX 20XX, Accepted Xth XXXXXXXXX 20XX
DOI: 10.1039/b000000x

This study evaluates the efficiency of novel non-viral vectors consisting of super paramagnetic iron oxide nanoparticles functionalized with the chemically tunable cationic polymer for *in vitro* gene magnetofection. The cationic polymer, poly(vinyl pyridinium alkyl halide), with reactive alkoxysilyl group at one terminal of the polymer (VPCm_n, m = length of the side chain, n = polymerization degree), was grafted onto the surface of iron oxide nanoparticles through a silane coupling reaction. The VPCm_n grafted-magnetic nanoparticles (Mag-VPCm_n) were quarternized with various alkyl halides such as methyl iodide (m =1), ethyl bromide (m = 2), butyl bromide (m = 4), hexyl bromide (m = 6) and octyl bromide (m = 8). Mag-VPCm_n quaternaized with shorter alkyl chain (m = 1, 2, 4 and 6) were water dispersible, but that quarternized with longer alkyl chain (m = 8) was precipitated in water. The surface of water dispersible Mag-VPCm_ns were positively charged in pH ranging from 2 to 11, and are stable for more than one month in this pH range. The complexes of Mag-VPCm_ns and nucleoside molecules with various N/P ratios were evaluated using gel electrophoresis, surface charge (ζ-potential) measurement, and particle size measurement. *In vitro* transfection experiments were assayed in human embryonic kidney 293 cells (HEK293 cells) using pmaxGFP plasmid as a reporter gene. Gene expression was found to be strongly influenced by the length of the side alkyl chains. Higher transfection efficiencies were observed with longer alkyl chains (C6 > C4 > C2 ≥ C1), indicating that hydrophobic side chains were effective in increasing transfection efficiency.

Introduction

Gene therapy is one promising technique to treat or prevent diseases.[1-4] The success of gene therapy is largely dependent on the development of viral or non-viral gene transfer vectors. In the last decade, magnetically guided gene transfection using magnetic nano-carriers[5-7] has attracted much attention due to its promising efficiency and simple and fast experimental process. The first report of magnetic nanoparticle guided gene transfection was reported by Mah's group.[8] They attached viral vectors to magnetic nanoparticles to achieve target-specific enhanced transfection, both *in vitro* and *in vivo*. An external magnetic field was applied to accumulate the magnetic nanoparticles containing the therapeutic genes onto the surface of the cells. Scherer et al.,[9] named the magnetic field-mediated transfection using magnetic particles 'magnetofection'. Since the first presentation on using magnetofection for gene delivery in 2002, the potential of this method to improve the delivery of plasmid DNA[10] and siRNA[11] in transgene expression has been extensively discussed in several articles. Most of the research reported so far regarding magnetic nanoparticle-mediated gene delivery suggests the simple mixing of the magnetic nanoparticles with cationic polymers such as polyethylenimine (PEI),[9,12] poly(lysine),[13] *N*-acylated chitosan,[14] cationic dendorimer,[15] polymethacrylate derivative[16], and cationic liposomes,[17] in order to coat the magnetic nanoparticles. Polyethylene imine (PEI), which is one of the most efficient non-viral polymer type gene delivery vectors[18] has been extensively investigated as a coating material of magnetic nanoparticles to improve transfection efficiency. PEI attached electrostatically on the surface of iron oxide nanoparticles, and the PEI-coated iron oxide nanoparticles forms complex with negatively charged DNA, siRNA, or nucleic acids. In general, PEI has a highly branched structure containing primary, secondary and tertiary amine groups. Therefore it is difficult to precisely control its chemical structure, which influences the nucleic acid transfection ability of this complex. The aim of this study is to develop chemically tunable cationic polymer-grafted magnetic nanoparticle carriers to investigate the effects of surface chemical structures of magnetic carriers on transfection efficiency. To realize this purpose, we synthesized poly(vinyl pyridine halide)-grafted magnetic nanoparticles (Mag-VPCm_n, shown in Scheme 1), in which the chemical structure can be accurately and facilely tuned by using various alkyl halides as quaternizing reagents. In the various cationic lipids and polymers that are employed as gene vectors, the cationic property and hydrophobic moiety are important factors in determining their transfection efficiency.[19] Thus, magnetic nanoparticles possessing a cationic charge and/or

comprising hydrophobic structures on their surface can make use of both electrostatic interaction and hydrophobic effect to capture virus particles into magnetic transfection vectors.[20]

Experiments

Materials

Unless otherwise noted, all chemicals for preparation and characterizations of cationic polymer-bonded magnetic nanoparticles were purchased from major suppliers such as Sigma-Aldrich Co., Kanto Chemical Co., Inc., Tokyo Chemical Industry Co., Ltd., Nacalai Tesque, Inc., and Wako Pure Chemical Industries, Ltd., and used as received. The plasmid pmaxGFP was used to assess the transfection efficiency.

Synthesis of cationic polymer-grafted magnetic nanoparticles (Mag-VPCm$_n$)

Magnetic nanoparticles: The magnetic nanoparticles (Mag) were prepared according to the method of Hyeon et al.[21] Briefly, 2 mL of $Fe(CO)_5$ was added to a mixture containing 100 mL of n-octyl ether and 12.8 g of oleic acid at 100°C. The resulting mixture was heated to reflux and kept at that temperature for 1 h. The resulting black solution was cooled to room temperature, and 3.4 g of dehydrated $(CH_3)_3NO$ was added. The mixture was then heated to 130°C under a nitrogen atmosphere and maintained at this temperature for 2 h. The reaction temperature was slowly increased to reflux, which was continued for 1 h. The solution was then cooled to room temperature, and ethanol was added to yield a black precipitate, which was then separated by centrifuging and dried *in vacuo*. The obtained slurry contained iron oxide nanoparticles and oleic acid. The crystal structure of iron oxide nanoparticles were examined by using an X-ray diffractometer (Rint2500HV, Rigaku Co., Japan).

Poly(4-vinylpyridine) with reactive group (Process A in Scheme 1): Poly(4-vinyl pyridine), VP$_n$, where n is the average degree of polymerization, with a terminal reactive group at the one end was prepared by modified telomerization method of 4-vinylpyridine with 3-mercaptopropyl trimethoxysilane.[22] Briefly, 4-vinylpyridine (10 mL, 94 mM), 3-mercaptopropyl trimethoxysilane (0.87 mL, 4.7 mM) and 100 mg of 2,2'-azoisobutyronitrile were mixed, and the mixture was stirred with bubbling N_2 gas at 60°C. After 3 h, the yellow colored product was dissolved in 15 mL of chloroform, and the solution was poured into 150 mL of diethyl ether to precipitate a pale yellow powder. Similar precipitation was repeated three times, and the collected powders were successively washed with diethyl ether and dried *in vacuo*. The yield was 8.5 g, 87%. The average degree of polymerization was determined by ^{1}H-NMR spectroscopy and characterized by NMR as: δH (400 MHz; $CDCl_3$; Me_4Si) 3.54 (9 H, s, $SiOCH_3$), 8.1-8.6 (42.35 H, m, 2- and 6-positions of pyridyl group).

Poly(4-vinylpyridine)-grafted magnetic nanoparticles (Process B in Scheme 1): VP$_n$ was grafted onto magnetic nanoparticles (Mag) by using the terminal trimethoxysilyl group. The slurry containing iron oxide nanoparticles (1.0 g, containing 38 wt% of iron oxide) and 1.5 g of VP$_n$ were added to a toluene/methanol (40 mL/10 mL) mixed solution, and the mixture was stirred gently at reflux temperature for 4 days. The obtained black precipitate was collected by centrifugation, washed successively with diethyl ether, and stocked in methanol. The amount of VP$_n$ immobilized on the Mag was determined by elemental analysis.

Alkylation of pyridyl groups on the Mag-VP$_n$ (Process C in Scheme 1): Excessive amount of alkyl halide (CmX: methyl iodide (C1I), ethyl bromide (C2Br), butyl bromide (C4Br), hexyl bromide (C6Br), and octyl bromide (C8Br)), were added to the Mag-VP$_n$ dispersion in methanol, and the dispersion was stirred at reflux temperature for 2 days. The magnetic nanoparticles obtained (Mag-VPCm$_n$) were corrected by centrifugation, washed with diethyl ether three times, and stocked in a water suspension. The alkylations (quaternizations) of pyridyl groups with alkyl halides were confirmed by diffuse reflectance infrared Fourier transform (DRIFT) spectroscopic measurements.

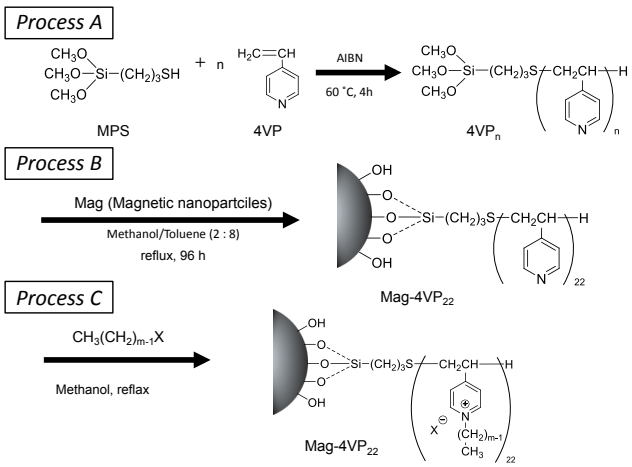

Scheme 1 Preparation procedure of Mag-VPCm$_n$.

Characterization of cationic polymer-grafted magnetic nanoparticles (Mag-VPCm$_n$)

The surface charges of Mag-VP$_n$ and Mag-VPCm$_n$ were measured by determination of z-potential using a Zetasizer Nano-ZS (Malvern Instruments, United Kingdom). Polymer-grafted magnetic nanoparticles prepared as described above were transferred onto a hydrophilic-treated copper grid, which was then rinsed with distilled water. Excess water was wicked off with filter paper and the grid was left overnight to dry out completely. The polymer-grafted magnetic nanoparticles were imaged by using transmission electron microscopy (TEM; JEOL-200FX, JEOL Co. Ltd., Japan).

Complex formation of Mag-VPCm$_n$ with gene

A gel retardation assay was performed as described below. Mag-VPCm$_{22}$/plasmid DNA complexes were prepared at various N/P ratios The N/P ratio is a value calculated by dividing the number of nitrogen residues (N) of Mag-VPCm$_{22}$ by the number of phosphate (P) in plasmid DNA). 0.55 mg/mL of plasmid DNA (pCMV bgal (7854 base pair), phosphate anion = 1.65 nmol/mL) was diluted in HEPES buffer (pH 7.6). 0.5 mg/mL of Mag-VPCm$_{22}$ aqueous dispersion was added to the plasmid DNA solution to be 0.5, 1, 2, 4, and 8 in the N/P ratio. The details of the preparation of mixtures were shown in Table S1. Mag-VPCm$_{22}$/plasmid DNA complexes were prepared at N/P ratio (the ratio of concentrations of nitrogen atoms (N) of Mag-VPCm$_{22}$ to phosphate groups (P) of plasmid DNA (7854 bp)) = 0.5, 1, 2, 4,

and 8. Plasmid DNA (0.55 mg, phosphate anion = 1.65 nmol/mL) was diluted in HEPES buffer (pH 7.6) and added to various amounts of Mag-VPCm$_{22}$. Mag-VPCm$_{22}$/plasmid DNA complexes and free plasmid DNA were incubated for 20 min at room temperature. The samples were electrophoresed on an agarose gel (1.0% wt) at 100 V for 45 min (Mupid-2, ADVANCE Co. Ltd., Japan). Following electrophoresis, the gels were then stained with ethidium bromide and visualized by the FAS III mini gel documentation system (Toyobo, Tokyo, Japan). The size and surface charge of the complexes were also evaluated by dynamic light scattering (DLS) and ζ-potential measurements, respectively.

Gene transfection efficiency of Mag-VPCm$_n$

Before transfection, HEK293 cells were seeded into individual wells. The 50μL of pmaxGFP aqueous solution (12 mg/L) was mixed with 50 μL of Mag-VPCm$_{22}$ aqueous solution with various N/P ratios (the ratio of number of nitrogen in Mag- VPCm$_{22}$ against that of phosphate in DNA), and the mixtures were incubated at room temperature for 20 min. After removing and discarding the culture medium, 100 μL of OptiMEM was added. Then 100 μL of each complex was added to the cells. The cells were incubated at 37°C in humidified-air (5% CO_2) for 1 h with and without the magnetic plate (OZ Biosciences), and then were incubated for another 2 h after removing the magnetic plate. Then, the OptiMEM and excess complex of plasmid and Mag-VPCm22 were removed, 200 μL of Dulbecco's modified Eagle's medium (DMEM) containing 10 % of Fetal Bovine Serum (FBS) was added to the cells, and the mixture was incubated for 60 h. The cells were observed by fluorescence microscope and the number of cells expressing GFP was counted.

Results and Discussion

Preparation of poly(*N*-alkyl-4-vinylpyridinium halide)-grafted magnetic nanoparticles (Mag-VPCm$_n$)

The magnetic nanoparticles were prepared by the conventional method with reduction of $Fe(CO)_5$ using oleic acid emulsion, according to a previous report.[21] The obtained magnetic nanoparticles were well-dispersed in organic solvents because their surface was covered with oleic acid. An X-ray diffraction spectrum (Figure 1d[15d]) indicates that the obtained particles mostly consist of iron oxide (Fe_3O_4 and γ-Fe_2O_3).[23] Broader peaks suggest that the particles are smaller in size.[24] TEM images indicate that the average particle diameter of magnetic nanoparticles is approximately 5 nm with narrow size distribution (Figure 1a). The magnetization curve of the obtained magnetic nanoparticles, Mag (as shown in Figure S3) indicated that the magnetization property is enough for the use in magnetofection. On the other hand, poly(4-vinyl pyridine) with the trimethoxysilyl group at one end (VP$_n$) was prepared by radical telomerization of 4-vinyl pyridine with 3-mercaptopropyl trimethoxysilane as a telogen. The polymerization degree of the obtained polymer was determined to be 22 using the integration ratio of the signals at 3.54 (9H, s, $SiOCH_3$) and 8.1-8.6 (42.4H, m, 2- and 6-positions of pyridyl group) ppm on the ^{1}H-NMR spectrum (Figure S1). The polymer, VP$_{22}$ was readily grafted onto the magnetic nanoparticles (Mag-VP$_{22}$) using the terminal trimethoxysilyl groups of VP$_{22}$. Terminal triethoxysilyl groups can connect to the surface Fe-OH groups of iron oxide through a covalent bond.[25] Mag contains 49% wt of carbon as shown in Table 1, indicating that the iron oxide nanoparticles are coated with oleic acid. After grafting of VP$_{22}$ onto Mag, the amount of nitrogen was definitely increased, and the observed C/N ratio of 6.27 was approximately the same as the calculated value of 6.12. These results suggest that the oleic acid can be removed from the surface of Mag-VP$_{22}$ by washing with ethanol. The DRIFT spectra (Figure S2) support this interpretation. The absorption band observed in the Mag around 1730 cm^{-1}, caused by the carbonyl group of the oleic acid, was absent in Mag-VP$_{22}$. Therefore the amount of polymer on Mag-VP$_{22}$ can be calculated as 72% wt using N% wt in the elemental analysis. The observed amount of hydrogen in the Mag and Mag-VP$_{22}$ were slightly larger than the calculated values. This is probably due to the Fe-OH groups that remained on the surface of the magnetic nanoparticles. TEM observation indicates that the morphology and size of magnetic nanoparticles were maintained even after VP$_n$ grafting (Figure 1b and 1c).

Table 1 Elemental analysis of Mag and Mag-VP$_{22}$.

		H%	C%	N%	C/N	Ash%
Mag	Found	8.09	48.86	0.09	-	37.9
	Calcd.	7.48	47.49	0.00	-	
VP$_{22}$	Found	6.78	73.16	11.88	6.16	0.0
	Calcd.	6.55	73.23	11.72	6.24	
Mag-VP$_{22}$	Found	5.40	58.02	9.26	6.27	28.0
	Calcd.	4.89	56.70	9.26	6.12	

Calcd. for Mag: iron oxide (38 wt%) and oleic acid (62 wt%).
Calcd. for Mag-VP$_n$: iron oxide (28 wt%) and VP$_n$ (72 wt%)

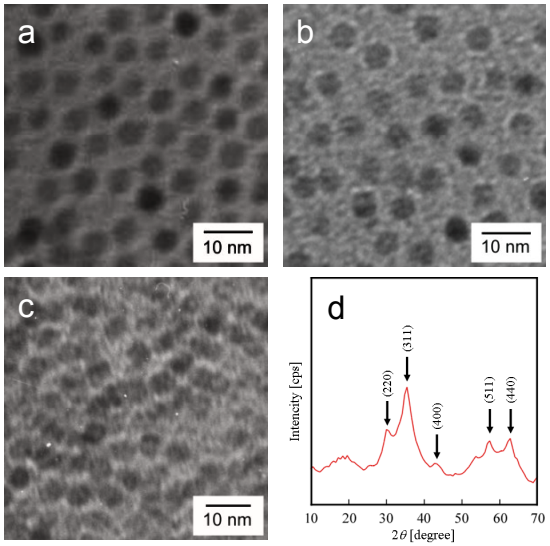

Figure 1 Transmission electron micrographs of a) Mag, b) Mag-(VP)$_{22}$ and c) Mag-VPC1$_{22}$, and d) X-ray diffraction pattern of Mag.

The pyridyl groups on Mag-VP$_n$ were alkylated (quarternized) with various alkyl halides. The DRIFT spectra of Mag-VP$_n$ (Figure 2) showed that the absorption band corresponding to the C=C stretching vibration at 1598 cm^{-1} shifted to a band at 1639 cm^{-1} after alkylation with the alkyl halides used in this study, indicating that the pyridyl groups were quaternaized (Mag-VPCm$_n$).

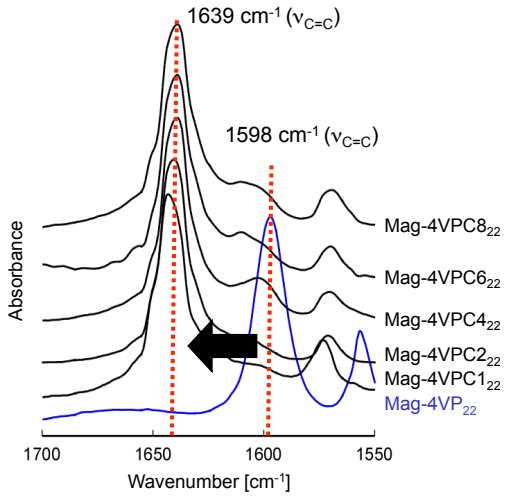

Figure 2 FT-IR spectra of Mag-VP_{22} and Mag-$VPCm_{22}$.

Aqueous dispersion of Mag-$VPCm_n$

All the Mag-$VPCm_{22}$, except Mag-$VPC8_{22}$, dispersed well in water, whereas Mag-VP_{22} did not disperse in water. Aqueous dispersions of Mag-$VPCm_{22}$ were stable, and no precipitations were observed for over than 6 months. Therefore, further investigations were carried out with Mag-$VPC1_{22}$, Mag-$VPC2_{22}$, Mag-$VPC4_{22}$, and Mag-$VPC6_{22}$. Surface charges of Mag-$VPCm_{22}$ were evaluated in aqueous dispersions. As shown in Figure 3, positive ζ-potentials were detected in aqueous solutions of Mag-$VPCm_{22}$ in a wide range of pH from 3 to 11, indicating that Mag-$VPCm_{22}$ dispersions are more stable in this pH range. The positively charged surface of Mag-$VPCm_{22}$ has the potential to absorb the negatively charged nucleobases.

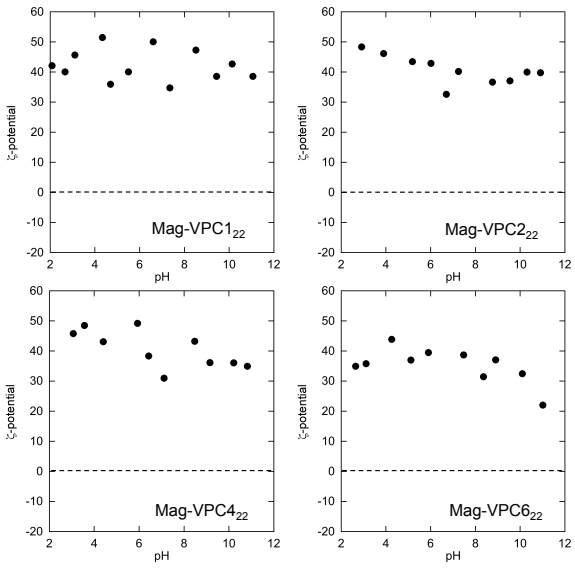

Figure 3 ζ-Potentials of Mag-$VPCm_{22}$/DNA complexes.

Complex formation of Mag-$VPC1_{22}$ with plasmid DNA

It has been predicted that the cationically charged pyridinium groups on Mag-$VPCm_{22}$ absorb anionically charged DNA. At first, the formation of the plasmid DNA and Mag-$VPCm_{22}$ complex was evaluated using agarose gel electrophoresis (Figure 4). In the images obtained from electrophoresis, the white bands signify the presence of ethidium bromide-stained plasmid DNA. When the plasmid DNA was tested on 1% agarose gel without any additives, the bands were observed near the positive pole. This indicates that the polymer network of the agarose gel is large enough for free plasmid DNA to migrate in the gel. However, by addition of Mag-$VPCm_{22}$, the migration behavior of plasmid DNA was gradually changed.

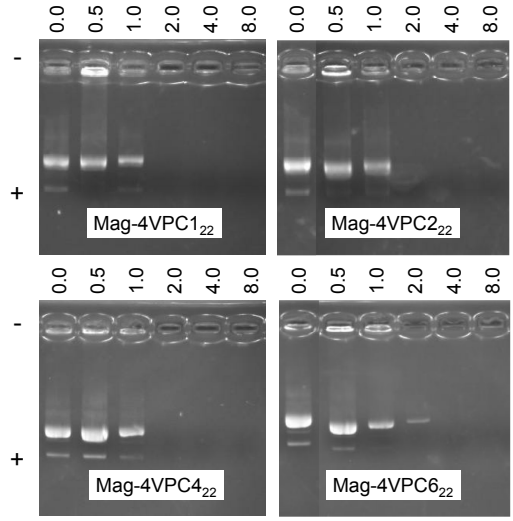

Figure 4 Agarose gel electrophoresis of Mag-$VPCm_{22}$/plasmid DNA complexes. The N/P ratio for each complexes is listed above the corresponding lane.

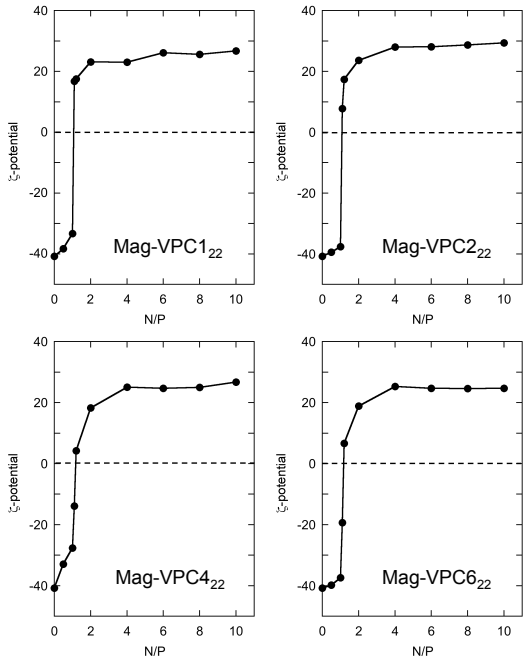

Figure 5 ζ-potentials of Mag-$VPCm_{22}$/plasmid DNA complexes.

Free plasmid DNA was observed at the N/P ratio of 0.5 and 1 for Mag-$VPC1_{22}$, Mag-$VPC2_{22}$, and Mag-$VPC4_{22}$, and at the N/P ratio of 0.5, 1, and 2, for Mag-$VPC6_{22}$. These results indicate that the longer side alkyl chains may be altered to form the complex with the plasmid DNA. The original spots at higher N/P ratios (2, 4, and 8) were darker than those at lower N/P ratios (0.5 and 1).

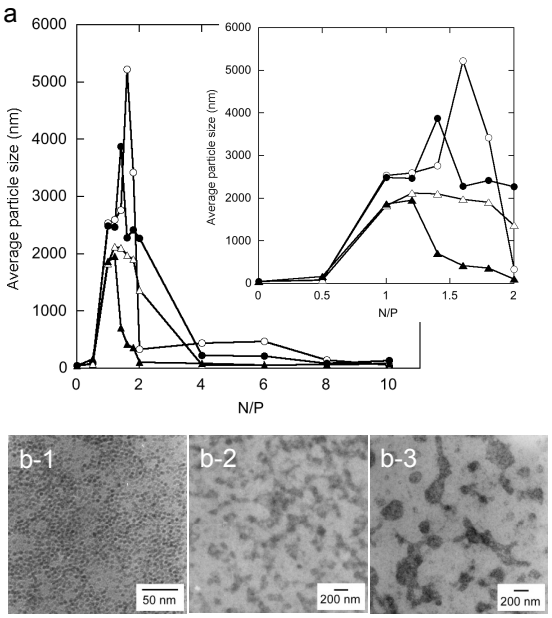

Figure 6 a) Average particle size and b) TEM images of the complexes of Mag-VPCm$_{22}$ with plasmid DNA. a) open circles: Mag-VPC1$_{22}$, closed circles: Mag-VPC2$_{22}$, open triangles: Mag-VPC4$_{22}$, closed triangles: Mag-VPC8$_{22}$; b-1) Mag-VPC1$_{22}$ alone, b-2) Mag-VPC1$_{22}$/plasmid DNA (N/P = 1), b-3) Mag-VPC1$_{22}$/plasmid DNA (N/P = 2).

This is probably due to a stronger complex formation with Mag-VPCm$_{22}$, which does not allow intercalation of ethidium bromide into DNA. These results were supported by ζ-potential measurements of the mixture of plasmid DNA with Mag-VPCm$_{22}$ (Fig. 5). Plasmid DNA is negatively charged in a phosphate buffer solution. The surface charges were drastically changed from negative to positive when mixed with Mag-VPCm$_{22}$.

In all complexes of Mag-VPCm$_{22}$ with plasmid DNA, the surface charges were reversed at around N/P = 1. The surface of the complexes at N/P = 1 were positively charged when mixed with Mag-VPC1$_{22}$ and Mag-VPC2$_{22}$, and negatively charged when mixed with Mag-VPC4$_{22}$ and Mag-VPC6$_{22}$. These results indicate that Mag-VPCm$_{22}$ with smaller side chains can form a tenacious complex with plasmid DNA. The complex formation of Mag-VPCm$_{22}$ and DNA was evaluated by DLS measurements with a commercially available DNA marker (7854 bp). The hydrodynamic size of DNA alone was approximately 50 nm, and the complex with Mag-VPCm$_{22}$ at N/P = 0.5 was increased slightly to 80-160 nm. As shown in Figure 5 the complexes were negatively charged at N/P = 0.5. These results indicate that when N/P ratio was less than 1, the DNA molecules probably covered the Mag-VPCm$_{22}$ to form a complex. The complex size increased drastically to more than 1 mm at N/P = 1 (point of electrical equivalence). These phenomena were confirmed by TEM observations. As shown in Figure 6b-1, it was clearly observed that Mag-VPC1$_{22}$ was well dispersed in the buffer solution, but formed agglomerated complexes with DNA molecules at N/P from 1 to 2 (or 4). Further addition of Mag-VPCm$_{22}$ reduced the complex size to approximately several tens nm. It is likely that Mag-VPCm$_{22}$ surrounds the DNA molecule to form stable complexes that may not agglomerate with each other because of their positively charged surface. The N/P ranges for the larger complexes are slightly different for each of the different Mag-VPCm$_{22}$s. For instance, the largest size can be observed around N/P = 1.6 in the complex with Mag-VPC1$_{22}$. But the complex size and their maximum range were lowered with an increase in the length of side alkyl chains (Mag-VPC1$_{22}$ > Mag-VPC2$_{22}$ > Mag-VPC4$_{22}$ > Mag-VPC8$_{22}$). At N/P = 4, the complex size reduced, with further reduction observed over N/P = 4. At N/P = 8, the average complex sizes were 146.7 nm (Mag-VPC1$_{22}$), 84.5 nm (Mag-VPC2$_{22}$), 71.4 nm (Mag-VPC4$_{22}$), and 74.5 nm (Mag-VPC6$_{22}$), respectively. In summary, all the Mag-VPCm$_{22}$s with different alkyl side chains formed complexes with DNA molecules, but their complex formation behaviors were imperceptibly different.

Effects of alkyl chain length of Mag-VPCm$_n$ on transfection efficiency and toxicity

As shown in Figure 7, GFP expression was observed in HEK293 cells after treatment with the pmaxGFP and Mag-VPCm$_{22}$ complexes. The transfection efficiency was affected by the side alkyl chains (Figure 8). When the complex systems of Mag-VPC1$_{22}$, Mag-VPC2$_{22}$, and Mag-VPC4$_{22}$ were transfected, the number of GFP-expressing cells increased with an increase in the N/P ratio of the complex and sharply increased at N/P = 8. In the Mag-VPC6$_{22}$ complex, the number of GFP-expressing cells was extremely enhanced compared to other systems, even at lower N/P ratios (0.5, 1, and 2). However, most cells were damaged at higher N/P ratios (4 and 8). When Mag-VPC6$_{22}$ was added to the incubated HEK293 cells, no serious damage was observed in the cells. This observation indicates that Mag-VPC6$_{22}$ in itself is not toxic, but the complex with the cationically charged surface is toxic. The detailed *in vitro* cytotoxicity was confirmed with CHO cells using MTT assay (Figure S4). The cationic liposomal system (*N,N*-di-n-hexadecyl-*N,N*-dihydroxyethylammonium chloride (DHDEAC) and co-lipid, cholesterol (Chol) at 1:1 molar ratio) was used as a reference. As shown in Figure S5, approximately 80% cells were viable with the cationic liposomal system (DNA : DHDEAC/Chol (the number of phosphate in plasmid DNA : the number of nitrogen residues of DHDEAC) = 1 : 1). Mag-VPCm$_{22}$ with methyl (m =1), ethyl (m =2) and butyl (m =4) side chains had negligible effects on the cell viabilities at the ratios from 1 : 0.5 : 1 to 1 : 8 : 1 (the number of phosphate in plasmid DNA : the number of nitrogen residues of Mag-VPCm$_{22}$: the number of nitrogen residues of DHDEAC). In comparison, Mag-VPCm$_{22}$ with hexyl (m = 6) side chains decreased cell viability at higher ratio of Mag-VPCm$_{22}$ ratios (1 : 4 : 1 and 1 : 8 : 1). These results agree with the observations of damaged cells in GFP expression measurements. By using a magnetic field during the transfection process, GFP expression is enhanced. As expected, hydrophobic side chains certainly affected gene transfection efficiency. In the present study, longer alkyl chains brought higher transfection efficiency regardless of the loading amount of Mag-VPC6$_{22}$. The observation of large differences in gene expression with small changes in the chemical structure of the vectors leads us to further investigations. In all the gene expression experiments with Mag-VPCm$_{22}$, it was observed that the use of the magnetic plate (OZ Biosciences, France) significantly enhanced the transfection efficiency.

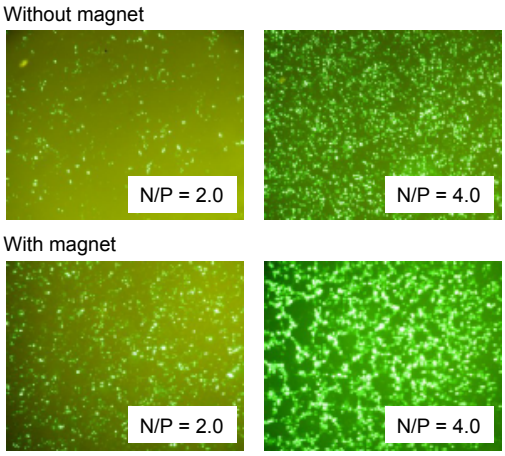

Figure 7 Expression of GFP in HEK 293 cells transfected with Mag-VPC6$_{22}$ seen through a fluorescence microscope. The upper row, fluorescence from cells incubated with magnet; the lower row, fluorescence from cells without magnet.

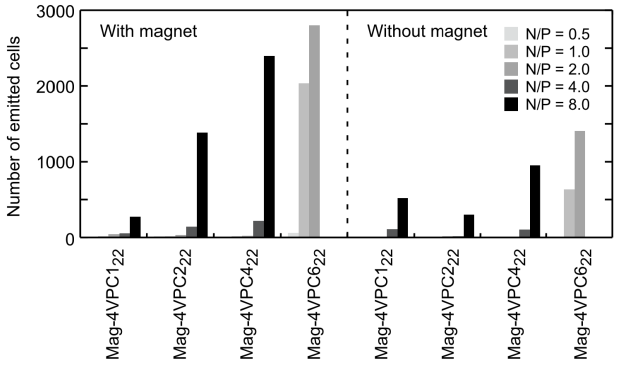

Figure 8 Transfection efficiencies of pmaxGFP to HEK293 cells with Mag-VPCm$_{22}$. The bar graphs show the number of GFP expression cells with magnet (left) and without magnet (right).

Conclusions

In this paper, we investigated the effects of the chemical structure of cationic polymer-bonded magnetic nanoparticles on the gene transfection efficiency by magnetofection. The transfection tests indicated that gene expression is strongly affected by the length of the side alkyl chains. Higher transfection efficiencies were observed with longer alkyl chains (C6 > C4 > C2 ≥ C1), indicating that hydrophobic side chains improve transfection efficiency. Transfection efficiencies were enhanced by the magnetic field. Since alkyl halides with various functional groups, such as hydrophilic, hydrophobic, and aromatic groups, are available for quarternization of pyridyl groups, this approach provides a series of systematic nanovectors with chemically tunable polymer-bonded magnetic nanoparticles.

Acknowledgements

This work was partially supported by the bilateral program between Japan Society for the Promotion of Science (Japan) and Department of Science and Technology (India). The authors greatly appreciate to Dr. N. M. Rao of Centre for Cellular and Molecular Biology (CCMB), India for his valuable advice on the magnetofection studies, and Dr. S. Morimura of Kumamoto University, Japan for his support to prepare plasmid DNA and measurements of gel electrophoresis.

Notes and references

[a] *Department of Applied Chemistry and Biochemistry, Kumamoto University, 2-39-1 Kurokami, Chuo-ku, Kumamoto 860-8555 Japan. Fax: +81-96-342-3662; Tel: +81-96-342-3661; E-mail: ihara@kumamoto-u.ac.jp*
[b] *Kumamoto Institute for Photo-Electro Organics (Phoenics), 3-11-38, Higashimachi, Higashi-ku, Kumamoto, 862-0901 Japan.*
[c] *CSIR-Centre for Cellular and Molecular Biology, Uppal Road, Hyderabad 500 007, Andhra Pradesh, India.*
[d] *The Chemo-Sero-Therapeutic Research Institute Kikuchi Research Center, 1314-1 Kyokushi, Kawabe, Kikuchi, Kumamoto 869-1298, Japan.*

† Electronic Supplementary Information (ESI) available: [details of any supplementary information available should be included here]. See DOI: 10.1039/b000000x/

‡ Footnotes should appear here. These might include comments relevant to but not central to the matter under discussion, limited experimental and spectral data, and crystallographic data.

1 S. Han, R. Mahato, Y. Sung and S. Kim, *Mol. Ther.*, 2000, **2**, 302.
2 D. W. Pack, A. S. Hoffman, S. Pun and P. S. Stayton, *Nat. Rev. Drug Discov.*, 2005, **4**, 581.
3 L. De Laporte, J. C. Rea, L. D. Shea, *Biomaterials,* 2006, **27**, 947.
4 J. E. Phillipsa, C. A. Gersbacha, A. J. Garcia, *Biomaterials*, 2007, **28**, 211.
5 J. Dobson, *Gene Ther.*, 2006, **13**, 283.
6 C. Plank, C, O. Zelphati, O. Mykhaylyk, *Adv. Drug. Deliv. Rev.*, 2011, **63**, 1300.
7 N. Laurent, C. Sapet, L. Le Gourrierec, E. Bertosio, O. Zelphati, *Ther. Deliv.*, 2011, **2**, 471.
8 C. Mah, T. J. Fraites, I. Zolotukhin, S. Song, T. R. Flotte, J. Dobson, C. Batich and J. Barry, *Mol. Ther.*, 2002, **6**, 106.
9 F. Scherer, M. Anton, U. Schillinger, J. Henkel, C. Bergemann, A. Kruger, B Gansbacher and C Plank, *Gene Ther.*, 2002, **9**, 102.
10 C. Sapet, N. Laurent, A. Chevigny, L. Gourrierec, E. Bertosio, O. Zelphati, C. Béclin, *BioTechniques*, 2011, **50**, 187.
11 a) O. Mykhaylyk, O. Zelphati, J. Rosenecker, C. Plank, *Curr. Opin. Mol. Ther.*, 2008 **10**, 493. b) R. Ensenauer, D. Hartl, J. Vockley, A. A. Roscher, U. Fuchs,, *Biotech. Histochem.*, 2011, **86**, 226. c) O. Mykhaylyk, O. Zelphati, E. Hammerschmid, M. Anton, J. Rosenecker, C. Plank, *Methods Mol. Biol.,* 2009, **487**, 111.
12 Y. Shi, J. Du, L. Zhou, X. Li, Y. Zhou, L. Li, X. Zang, X. Zhang, F. Pan, H. Zhang, Z. Wang, X. Zhu, *J. Mater. Chem.*, 2012, **22**, 355.
13 M. Hashimoto, Y. Hisano, *J. Neurosci. Meth.*, 2011, **194**, 316.
14 S. R. Bhattarai, S. Y. Kim, K. Y. Jang, K. C. Lee, H. K. Yi, D.Y. Lee, H. Y. Kim, P. H. Hwang, *Nanomed. Nanotechnol. Biol. Med.*, 2008, **4**, 146.
15 a) B. Pan, D. Cui, Y. Sheng, C. Ozkan, F. Gao, R. He, Q. Li, P. Xu, T. Huang, *Cancer Res.*, 2007, **67**, 8156. b) W. Liu, Y. Xue, N. Peng, W. He, R. Zhuo, S. Huang, *J. Mater. Chem.*, 2011, **21**, 13306. c) B. González, E. Ruiz-Hernández, M. J. Feito, C. L. Laorden, D. Arcos, C. Ramírez-Santillán, C. Matesanz, M. T. Portolés, M. Vallet-Regí, *J. Mater. Chem.*, 2011, **21**, 4598.
16 S. Huang, J. Ke, G. Chena, L. Wang, *J. Mater. Chem. B*, 2013, **1**, 5916.
17 a) A. Ito, T. Takahashi, Y. Kameyama, Y. Kawabe, M. Kamihira, *Tissue Eng. Part C Methods*, 2009, **15**, 57. b) Y. Namiki, T. Namiki, H. Yoshida, Y. Ishii, A. Tsubota, S. Koido, K. Nariai, M. Mitsunaga, S. Yanagisawa, H. Kashiwagi, Y. Mabashi, Y. Yumoto, S. Hoshina, K. Fujise, N. Tada, *Nat. Nanotechnol.*, 2009, **4**, 598. c) X. Zheng, J. Lu, L. Deng, Y. Xiong, J. Chen, *Int. J. Pharm.*, 2009, **366**, 211. d) S. Govindarajan, K. Kitaura, M. Takafuji, H. Ihara, K. S. Varadarajan, A. B. Patel, V. Gopal, *Int. J. Pharmaceutics*, 2013, **446**, 87.
18 a) S. Kadota, T. Kanayama, N. Miyajima, K. Takeuchi, K. Nagata, *J. Virol. Meth.*, 2005, 128, 61. b) T. Buerli, C. Pellegrino, K. Baer, B. Lardi-Studler, I. Chudotvorova, J.M. Fritschy, I. Medina, C. Fuhrer,

Nat. Protoc., 2007, **2**, 3090. c) Y. Shi, L. Zhou, R. Wang, Y. Pang, W. Xiao, H. Li, Y. Su, X. Wang, B. Zhu, X. Zhu, D. Yan, H. Gu, *Nanotechnology*, 2010, **21**, 115. d) R. Namgung, K. Singha, M.K. Yu, S. Jon, Y.S. Kim, Y. Ahn, I.K. Park, W.J. Kim, *Biomaterials*, 2010, **31**, 4204. e) B. Steitz, H. Hofmann, S.W. Kamau, P.O. Hassa, M.O. Hottiger, B. von Rechenberg, M. Hofmann-Amtenbrink, A. Petri-Fink, *J. Magn. Magn. Mater.*, 2007, **311**, 300.

19 a) K. Agopian, B.L. Wei, J.V. Garcia, D. Gabuzda, *J. Virol.*, 2006, **80**, 3050. b) Q. G. Li, K. Lindman, G. Wadell, *Arch. Virol.*, 1997, **142**, 1307.

20 a) A. Hofmann, D. Wenzel, U. M. Becher, D. F. Freitag, A. M. Klein, D. Eberbeck, M. Schulte, K. Zimmermann, C. Bergemann, B. Gleich, W. Roell, T. Weyh, L. Trahms, G. Nickenig, B. K. Fleischmann, A. Pfeifer, *Proc. Natl. Acad. Sci. USA*, 2009, **106**, 44. b) C. Orlando, S. Castellani, O. Mykhaylyk, E. Copreni, O. Zelphati, C. Plank, M. Conese, *J. Gene Med.*, 2010, **12**, 747. c) N. Tresilwised, P. Pithayanukul, O. Mykhaylyk, P.S. Holm, R. Holzmuller, M. Anton, S. Thalhammer, D. Adiguzel, M. Doblinger, C. Plank, *Mol. Pharm.*, 2010, **7**, 1069.

21 T. Hyeon, S. S. Lee, J. Park, Y. Chung, H. B. Na, *J. Am. Chem. Soc.,* 2001*,* **123**, 12798.

22 M. Takafuji, T. Mimaki, Z. Xu, H. Ihara, *J. Nanosci. Nanotechnol.*, 2005, **5**, 390.

23 J. Park, E. Lee, N. M. Hwang, M. Kang, S. C. Kim, Y. Hwang, J. H. Park, T. Hyeon, *Angew. Chem. Int. Ed.*, 2005, **117**, 2872.

24 a) W. Cheng, K.Tang, Y. Qi, J.Sheng, Z.Liu, *J. Mater. Chem.*, 2010, **20**, 1799. b) J. S. Son, K. Park, M. K. Han, C. Kang, S. G. Park, J. H. Kim, *Angew. Chem. Int. Ed.*, 2011, **50**, 1363.

X. Huang, A. Schmucker, J. Dyke, S. M. Hall, J. Retrum, B. Stein, N. Remmes, D. V. Baxter, B. Dragnea and L. M. Bronsteina, *J. Mater. Chem.*, **2009**, 19, 4231.